CHEMISTRY
AN ASIAN JOURNAL

DOI: 10.1002/asia.200600385

Folding Dynamics of 10-Residue β-Hairpin Peptide Chignolin

Atsushi Suenaga,* Tetsu Narumi, Noriyuki Futatsugi, Ryoko Yanai, Yousuke Ohno, Noriaki Okimoto, and Makoto Taiji*[a]

Abstract: Short peptides that fold into β-hairpins are ideal model systems for investigating the mechanism of protein folding because their folding process shows dynamics typical of proteins. We performed folding, unfolding, and refolding molecular dynamics simulations (total of 2.7 μs) of the 10-residue β-hairpin peptide chignolin, which is the smallest β-hairpin structure known to be stable in solution. Our results revealed the folding mechanism of chignolin, which comprises three steps. First, the folding begins with hydrophobic assembly. It brings the main chain together; subsequently, a nascent turn structure is formed. The second step is the conversion of the nascent turn into a tight turn structure along with interconversion of the hydrophobic packing and interstrand hydrogen bonds. Finally, the formation of the hydrogen-bond network and the complete hydrophobic core as well as the arrangement of side-chain–side-chain interactions occur at approximately the same time. This three-step mechanism appropriately interprets the folding process as involving a combination of previous inconsistent explanations of the folding mechanism of the β-hairpin, that the first event of the folding is formation of hydrogen bonds and the second is that of the hydrophobic core, or vice versa.

Keywords: beta-hairpin · chignolin · molecular dynamics · protein folding · protein structures

Introduction

The protein-folding problem of how a chain of amino acids folds into a well-defined unique protein structure is one of the most fundamental questions in the biosciences. Although a typical protein has numerous conformations, which makes a thorough search for the native structure in the global-minimum free-energy state difficult, protein folding is known to be a rapid process. The characterization of the folding dynamics and free-energy landscape of proteins is an important step not only in understanding the protein-folding mechanism, but also in solving the abovementioned paradox. The elucidation of these properties of protein elements, such as α-helices and β-hairpins, provides us with information about the early events of the protein-folding process. β-Hairpins are the simplest models for protein-folding study because they exhibit much characteristic behavior in the typical folding dynamics of proteins, such as the two-state transition.[1–4] In the past few years, the folding dynamics and energetics of a variety of β-hairpin systems have been well-studied experimentally[1–11] and theoretically.[12–31] These studies reported that β-hairpin folding occurs on a microsecond timescale,[4–7,9–11] which is slower than the rate of formation of the other typical protein elements such as the α-helix.[32,33] This means that they can be assessed both by fast time-resolved experiments and by computer simulations that use the latest high-performance computers to follow the entire folding process. Therefore, a complete picture of the folding mechanism can be obtained by combining the experimental and theoretical findings.[23,34,35]

Although previous experimental and theoretical studies generally support the idea that the peptide sequence is an important determinant of the folding of β-hairpins, many predictions are yet to be demonstrated; hence, a solid conclusion of the folding mechanism of the β-hairpin has remained elusive. For example, it is still under debate whether β-hairpin folding begins with the formation of a turn,[3,4,16,24] an interstrand hydrogen bond,[29] or hydrophobic collapse;[12,14,17–20] the rate-limiting step may also correspond to the formation of a sufficient number of interstrand con-

[a] Dr. A. Suenaga, Dr. T. Narumi, Dr. N. Futatsugi, R. Yanai, Dr. Y. Ohno, Dr. N. Okimoto, Dr. M. Taiji
High-Performance Molecular Simulation Team
Computational and Experimental System Biology Group
RIKEN Genomic Sciences Center
61-1 Ono-cho, Tsurumi, Yokohama, Kanagawa 230-0046 (Japan)
Fax: (+81)45-507-2524
E-mail: suenaga@gsc.riken.jp
taiji@gsc.riken.jp

tacts,[15] critical hydrophobic contacts,[3,4] or turns.[6,28] Therefore, it is quite interesting to follow the entire folding kinetics of the β-hairpin at the atomic-resolution level, in which molecular dynamics (MD) simulation is a very powerful tool. Recently, effective extended ensemble MD simulations, such as the replica-exchange method and the multicanonical ensemble method, have been widely used to escape local-minimum problems and to figure the free-energy landscape of proteins. On the other hand, the conventional canonical or microcanonical MD simulation provides us with the kinetic aspects directly. Although large-scale distributed computer simulation in the form of many short canonical MD simulations is one of the most effective techniques,[36,37] it is of great interest and very important to perform the long-timescale canonical MD simulation to study the protein-folding problem.

Herein, we performed a series of long-timescale canonical MD simulations of a designed peptide named chignolin (consisting of 10 amino acid residues) in an explicit solvent to follow its entire folding process in atomistic detail. Chignolin is the smallest β-hairpin known to be stable in solution (Figure 1).[2] Although the folding rate of chignolin has not yet been measured, the 10-residue chignolin is believed to fold into a β-hairpin on a timescale of nanoseconds or a few microseconds, because of its small size and high foldability regardless of the surrounding context.[2] MD simulations of chignolin, therefore, are expected to provide us with complete information about its folding dynamics at the atomic level.

Owing to the complexity of the representation and the demand for a huge number of steps to follow the entire folding process by conventional canonical MD simulation, such simulations have been, to date, limited to about a microsecond or less (single MD simulation for the system including about 10000 atoms).[38] To overcome this limitation, we developed a special-purpose computer for the MD simulation, MDGRAPE-3, which functions with high speed and accuracy.[39–41] We constructed a Petaflops system, which is a cluster of personal computers each equipped with the MDGRAPE-3. The Petaflops system enables us to perform MD simulations of a small or large protein with an accumulation time of 1 ms or 1 μs, respectively, on a practical timescale. Thus, the Petaflops system is a powerful computer system not only for long-timescale single MD simulation but also for massive parallel simulation. In this study, we used MDGRAPE-3 (only one MDGRAPE-3 board; two Tflops)

Abstract in Japanese:

βヘアピン構造に折りたたむ短いペプチド鎖は、タンパク質折りたたみの研究において最適なモデルシステムである。我々は、１０残基という短いペプチド鎖でβヘアピン構造をとるシニョリンの折りたたみ・熱変性・巻き戻りの分子動力学シミュレーションを行いその動態を観察した。その結果、シニョリンは、３段階の過程を経て折りたたむことが示唆された。

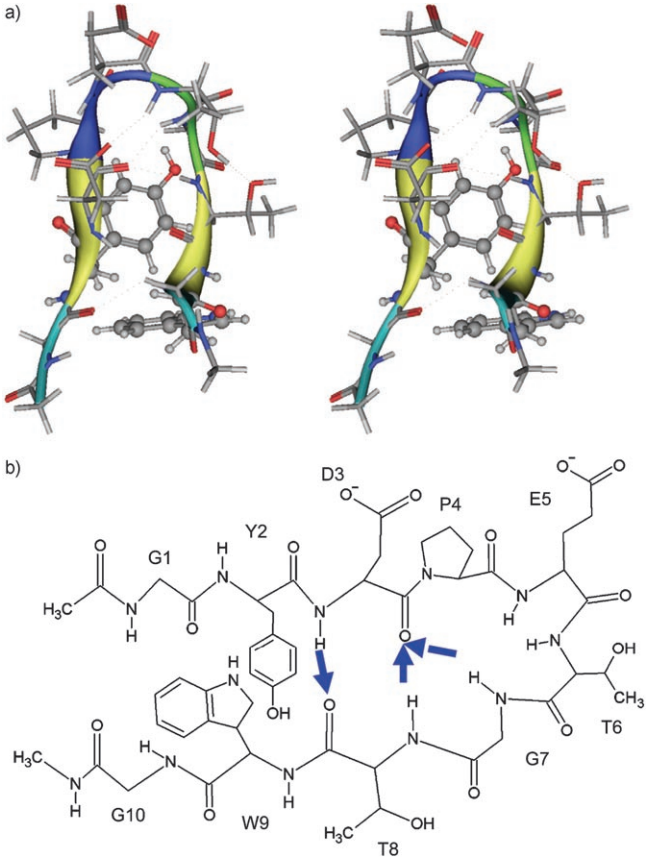

Figure 1. Structure of chignolin. a) Stereoview of chignolin. The backbone is represented by a ribbon model. The side chains of Tyr2 and Trp9 are highlighted by ball-and-stick models. b) Schematic representation of chignolin showing the pattern of hydrogen bonds from the backbone nitrogen atom to the backbone oxygen atom (direction of the arrows).

to reveal the folding mechanism of a peptide prior to that of a small protein.

Results and Discussion

Standard Check

We performed a series of MD simulations of chignolin (Table 1). To verify the stability of the native state in our simulation method, we first carried out an MD simulation at

Table 1. Summary of simulations.

Simulation	Initial structure	T [K]	Simulation time [μs] (No. of atoms)
NMR	Solution structure[a]	277	0.5 (3762)
Unfolding	Solution structure[a]	373	0.2 (10161)
Refolding	Unfolded structure[b]	277	0.6 (10161)
Folding	Fully extended structure	277	0.4 (7515[c])
Helix	Fully helical structure	277	1.0 (7212)

[a] Solution structure was obtained from the Protein Data Bank (PDB ID: 1UAO). [b] Unfolded structure was obtained from the unfolding simulation (a snapshot at 65 ns). [c] This value indicates the system size after removal of excess water molecules. The initial system for the folding simulation consisted of 11283 atoms.

277 K by using the solution structure; this structure was previously determined by NMR spectroscopy at 277 K.[2] In this simulation, chignolin was very stable and maintained a β-hairpin structure during the 0.5-μs simulation, which is consistent with the results of the NMR experiment[2] ((0.82 ± 0.14) Å main-chain root-mean-square deviation (RMSD) from the structure obtained by NMR spectroscopy, data not shown).

In our simulations, the peptides were immersed in the spherical water droplet, and water molecules at the surface of the droplet were constrained with a harmonic potential to prevent diffusion of the water molecules into vacuum. Prior to this study, we investigated how the size of the water sphere influences the structure and dynamics of the protein and the dynamics of the solvent water molecules. We explain these results briefly here (unpublished data and not shown here).

The effect of the size of the water sphere was investigated in solvent depths of 9 to 27 Å. We found that the water-sphere system with a solvent depth of 9 Å heavily influenced the structural and dynamic properties of proteins, and these properties were not supported by experimental data. On the other hand, water-sphere systems with a solvent depth beyond 15 Å showed similar behavior in protein structure and dynamics, and this time the properties are consistent with experimental data. Accordingly, from the viewpoint of the structure and dynamics of proteins in water droplets, it was proved that the water-sphere system with a solvent depth of at least 15 Å was required for accurate representation of the protein dynamics. Furthermore, we analyzed the water-droplet radial distribution as a function of distance from the protein surface. In the water-sphere system with a solvent depth of 9 Å, the first peak in the MD simulation was higher than those of the larger water-sphere systems, and the second peak appeared closer to the protein surface than those of larger systems; the radial distributions of the larger water-sphere systems showed similar behavior. Next, we investigated in detail the diffusion coefficient of solvent water molecules around the protein. As a result, it became clear that solvent water molecules positioned beyond 11–12 Å from the protein surface behaved as bulk water molecules in the systems with solvent depths of over 15 Å. These findings suggest that a harmonic boundary potential to prevent evaporation of the solvent water molecules would not give immensely high pressure within a droplet with a solvent depth over 15 Å. From these results, we judged that the solvent depth of the water-sphere system has to be greater than 15 Å to give the valid dynamic properties of protein and solvent water molecules. The water-sphere systems used in this study satisfied this condition. Therefore, our simulations provided fully reliable kinetics of protein folding. Besides these results, the validity of the simulation by using the spherical water droplet has also been shown by other folding simulations.[42,43]

Folding and Refolding Process

Next, we performed the folding and refolding simulations of chignolin by using the fully extended or unfolded structures to elucidate its folding process. The unfolded structure, in which the native structure was fully disrupted with a main-chain RMSD of 6 Å, was obtained from the unfolding simulation at 65 ns (see below and Figure 2). The 10-residue extended or unfolded chignolin folded into the β-hairpin conformation within 0.4 μs in the folding simulation or within 0.6 μs in the refolding simulation (Figures 2–4). In the (re)-folding process, the radius of gyration initially decreased from 8 to 6 Å (Figures 3b and 4b), but it was still larger than in the native structure (5 Å). In the initial collapse stage, the solvent-accessible surface area (SASA) of the hydrophobic residues and the distance between the two hydrophobic residues, namely, Tyr2 and Trp9, decreased with considerable fluctuations (Figures 3c,d and 4c,d), indicating a weak hydrophobic assembly. This brought the main chain together; subsequently, a nucleus of turn structure was formed in the region of residues 4–7 (Figures 3e and 4e). The weak packing of these hydrophobic side chains and the

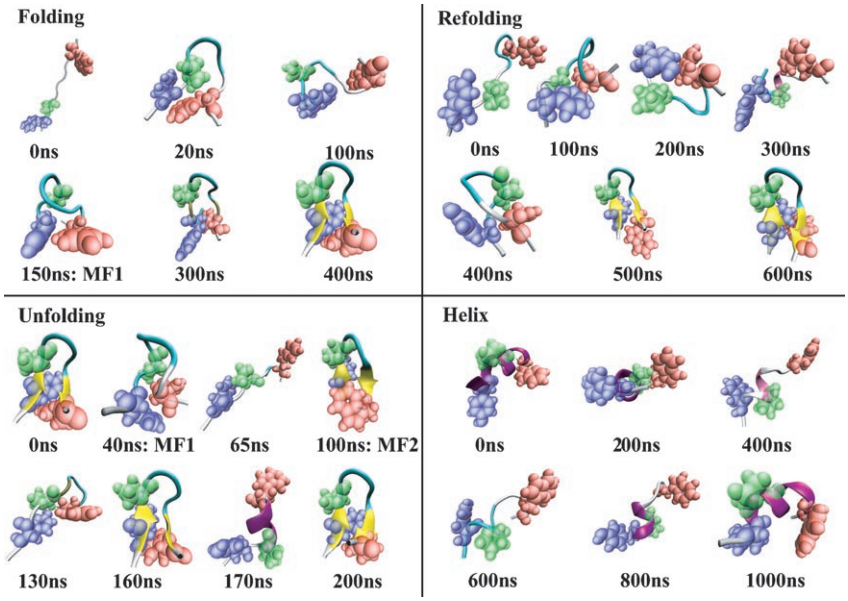

Figure 2. Snapshots from the folding, refolding, unfolding, and helix simulations. Three hydrophobic residues, Tyr2 (blue), Pro4 (green), and Trp9 (red), are represented by space-filled models. The α-helix, β-sheet, and turn structures are in magenta, yellow, and cyan, respectively. MF1 and MF2 = misfolded structures, F = folded structure.

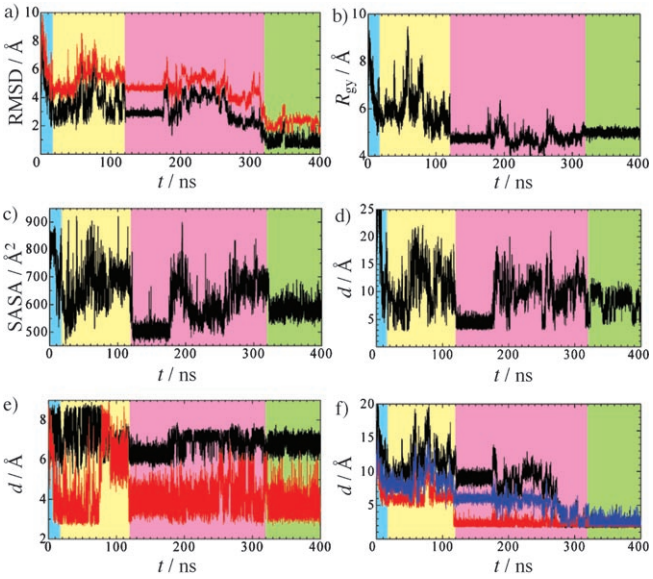

Figure 3. Results of the folding simulation. Time courses of the a) RMSDs of the main chain (black) and all atoms (red) from the solution structure, b) radius of gyration, c) SASA of the hydrophobic residues, d) distance between the two hydrophobic residues C_{ζ}(Tyr2) and $N_{\varepsilon}1$(Trp9), e) O(Tyr2)–N(Glu5) (corresponding to turn 2–5; black) and O(Pro4)–N(Gly7) distances (corresponding to turn 4–7; red), and f) distances between donor and acceptor atoms of the three interstrand hydrogen bonds O(Asp3)···H(Thr8) (blue), O(Asp3)···H(Gly7) (red), and H-(Asp3)···O(Thr8) (black). Blue region = formation of the hydrophobic assembly and nascent turn structure, yellow region = formation of the tight turn, pink region = formation of the hydrogen-bond network and complete hydrophobic core as well as arrangement of side-chain–side-chain interactions, green region = the native state.

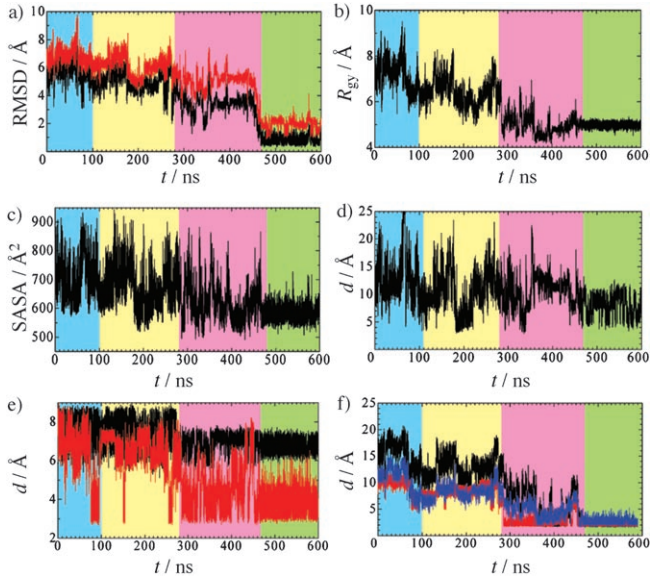

Figure 4. Results of the refolding simulation. Time courses of the a) RMSDs of the main chain (black) and all atoms (red) from the solution structure, b) radius of gyration, c) SASA of the hydrophobic residues, d) distance between the two hydrophobic residues C_{ζ}(Tyr2) and $N_{\varepsilon}1$(Trp9), e) O(Tyr2)–N(Glu5) (corresponding to turn 2–5; black) and O(Pro4)–N(Gly7) distances (corresponding to turn 4–7; red), and f) distances between donor and acceptor atoms of hydrogen bonds O-(Asp3)···H(Thr8) (blue), O(Asp3)···H(Gly7) (red), and H(Asp3)···O-(Thr8) (black). Color regions are as in Figure 3.

nascent turn formation were driving forces for the collapse. The first collapse stage was completed after 0.02 and 0.10 μs in the folding and refolding simulations, respectively. The importance of the collapse in the early stage of the β-hairpin folding process was consistent with theoretical and experimental observations, which indicates that, relative to helical proteins, a more significant collapse precedes the formation of the secondary structure during the folding of the β-sheet proteins.[44,45]

Following the collapse stage, a tight turn, which was observed in the native structure, was formed in the region of residues 4–7 (turn 4–7) from the nascent turn along with interconversion of the hydrophobic packing and interstrand hydrogen bonds (Figures 3c–f and 4c–f). The duration of this stage (tight-turn formation) was 0.02–0.12 μs in the folding simulation and 0.10–0.28 μs in the refolding simulation.

Turn 4–7 appears to be crucial for β-hairpin formation. This is because once turn 4–7 is formed, it persists throughout the folding and refolding simulations. Furthermore, in the helix simulation, the artificial helical structure on the sequence of chignolin fluctuated considerably; however, only the N terminus single-coiled helix (residues 2–5; a type of turn structure, turn 2–5) remained stable (Figures 2 and 5). Moreover, the helical structure was not converted into the β-hairpin in 1.0 μs, which is two times longer than the folding time of chignolin estimated from our simulations

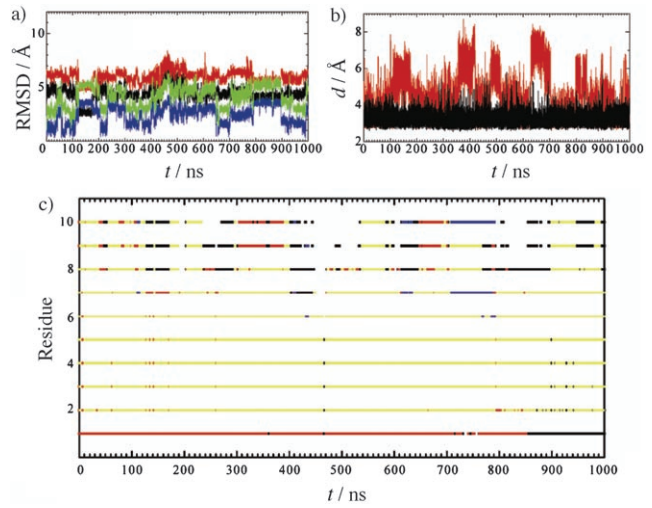

Figure 5. Results of the helix simulation. Time courses of the a) RMSDs of the main chain (black = NMR simulation, blue = helix simulation) and all atoms (red = NMR simulation, green = helix simulation) from the solution structure, b) O(Tyr2)–N(Glu5) (corresponding to turn 2–5; black) and O(Pro4)–N(Gly7) distances (corresponding to turn 4–7; red), and c) profile of the secondary structure. Each secondary structure was assigned by DSSP (definition of the secondary structure of proteins).[49] Red = α-helix, yellow = 3_{10}-helix, blue = β-bridge, black = turn structure.

(≈0.5 μs). These results indicate that turn 2–5 is a key configuration for the helical structure and hinders the path of β-hairpin formation. In our simulations, the sequence of chignolin favored turn 4–7 rather than turn 2–5 in the early

CHEMISTRY
AN ASIAN JOURNAL

stage of the folding process due to the presence of an energy barrier (potential of mean force (PMF) ≈ 4.5 kcal mol^{-1}) in forming turn 2–5 (Figure 6). This is possibly why

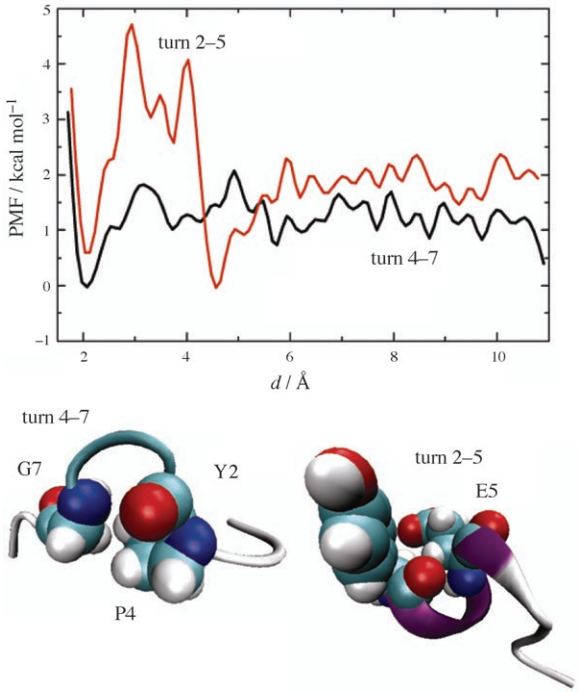

Figure 6. Calculated PMFs for the formation of turn 2–5 and turn 4–7 as a function of the distance between O(Tyr2) and N(Glu5) (turn 2–5) and O(Pro4) and N(Gly7) (turn 4–7).

chignolin has the β-hairpin and not the helical structure. The finding that the turn structure is a key factor in β-hairpin folding is supported by theory[46] and experiment,[5,6,9] in which even a difference of one residue in the turn region can change the refolding kinetics of a β-hairpin peptide. Thus, the turn sequence is a strong determinant of the folding rate of β-hairpins.

After the formation of the tight turn, the peptide was tightly packed; the radius of gyration decreased to about 5 Å. In this stage, the peptide became compact; this structure is similar to the native but not the β-hairpin structure (Figures 3a,b and 4a,b). While in the conformational space of the incomplete compact structures with various native interactions available (e.g., hydrogen bonds, hydrophobic interactions, and side-chain packing), the peptide visited the misfolded state (MF1) with short lifetimes (0.120–0.170 μs in the folding simulation) (Figures 2 and 3). The remarkable characteristics of MF1 are its rigidity (Figure 3) and the atypical hydrophobic interaction, which is the face-to-face interaction of the two aromatic rings of Tyr2 and Trp9 (parallel orientation of rings) (Figure 7). In the solution structure, these aromatic rings exhibit edge-to-face interaction (rings are perpendicular to each other).[2] For the conformation to escape the misfolded state, the peptide undergoes unfolding of the misfolded structure while maintaining its

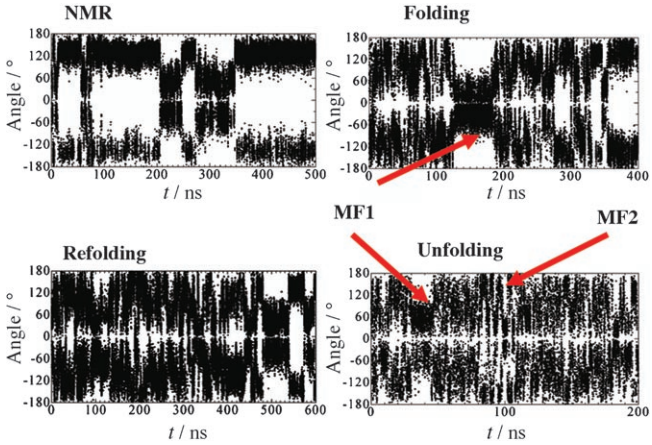

Figure 7. Time evolutions of the angle between the aromatic rings of Tyr2 and Trp9 obtained by the various simulations. Three carbon atoms from the aromatic ring are used to define the plane of the ring.

compactness (Figures 2 and 3). The existence of the misfolded structure caused by the atypical hydrophobic interaction was also predicted by computer simulation of a Trp cage.[47]

Finally, formation of the native hydrogen bonds and the complete hydrophobic core as well as arrangement of the side-chain packing occurred simultaneously (Figures 2–4). The two aromatic rings were stably located in the edge-to-face position (Figure 7), and the peptide then folded into the complete β-hairpin structure. The duration of this final stage was 0.12–0.32 μs in the folding simulation and 0.28-0.47 μs in the refolding simulation. Taken together, the folding of chignolin occurs mainly in three steps: 1) hydrophobic assembly and formation of the nascent turn structure, 2) tight-turn formation, and 3) formation of the native hydrogen bonds and hydrophobic core as well as arrangement of side-chain–side-chain interactions at approximately the same time. This mechanism was well-reproduced in both folding and refolding simulations (Figures 2–4). The folding time constant of about 0.5 μs is larger than the (1.0 ± 0.3) μs predicted by van der Spoel and Seibert,[48] because our analysis of folding events observed from our simulations were statistically poor.

Unfolding Process

Whether the unfolding process of chignolin is a reverse of the folding process is an interesting problem. In the unfolding simulation at 373 K with the solution structure, the unfolding of chignolin initiated a break in the hydrogen bonds, side-chain–side-chain interactions, and the hydrophobic core in 0.018 μs (Figures 2 and 8); this is the reverse of the folding process. After the initial step, the unfolded chignolin maintained relatively compact conformations (Figures 2 and 8). The conformational space of these incomplete compact structures was spread widely. In the unfolded chignolin conformations, both hydrophilic and hydrophobic interactions were maintained to some extent, although the native hydrogen bonds, local hydrophobic interactions, and side-chain

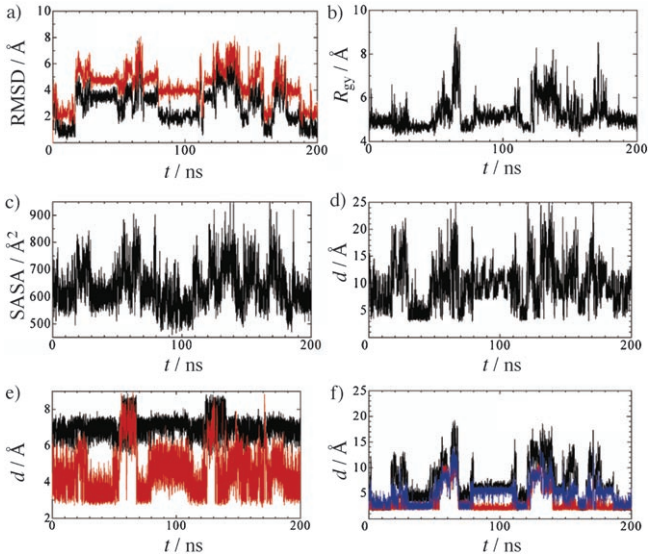

Figure 8. Results of the unfolding simulation. Time courses of the a) RMSDs of the main chain (black) and all atoms (red) from the solution structure, b) radius of gyration, c) SASA of the hydrophobic residues, d) distance between the two hydrophobic residues C_ξ(Tyr2) and N_ε1(Trp9), e) O(Tyr2)–N(Glu5) (corresponding to turn 2–5; black) and O(Pro4)–N(Gly7) distances (corresponding to turn 4–7; red), and f) distances between donor and acceptor atoms of the three interstrand hydrogen bonds O(Asp3)···H(Thr8) (blue), O(Asp3)···H(Gly7) (red), and H-(Asp3)···O(Thr8) (black).

packing were broken (Figure 8). This result was consistent with both the experimental observation that a residual fraction of the interactions persisted even at the boiling point of water or in the presence of concentrated denaturant,[2] and with the results of the previous unfolding simulation of the β-hairpin.[20] Among the three native hydrogen bonds, O-(Asp3)···H(Gly7) was more stable than O(Asp3)···H(Thr8) and H(Asp3)···O(Thr8) in the unfolding simulation (Figure 8 f). Moreover, in our folding and refolding simulations, O(Asp3)···H(Gly7) was formed faster than the other native hydrogen bonds (Figures 3 f and 4 f). Thus, O(Asp3)–H-(Gly7) is the strongest among the three native hydrogen bonds. These results are supported by those of the multicanonical MD simulation of chignolin[31] and an amide H–D exchange experiment, in which the protection factor for H_N at Gly7 was large.[2]

From 0.029 to 0.045 μs, the unfolded chignolin visited the misfolded state, which is similar to that shown in the folding simulation (MF1; Figures 2, 7, and 8). At 0.065 μs in the unfolding simulation, the unfolded chignolin became an extended structure, which is a minor conformation among the various unfolded conformations (Figures 2 and 8). From 0.080 to 0.108 μs, the unfolded chignolin again visited another misfolded state (MF2; Figures 2 and 8). In MF2, only the side-chain packing was lost, in particular, the two aromatic rings that were atypically positioned (Figures 2 and 8). These two misfolded states caused by atypical hydrophobic packing (MF1 and MF2) may not be the intermediate states during the folding–unfolding process because they have a short lifespan and were not observed in the refolding simulation, thus indicating that passage through these misfolded states is not an essential step for the folding process. After 0.155 μs, the unfolded chignolin refolded into a β-hairpin structure, which again unfolded at 0.171 μs and further refolded at 0.187 μs (Figures 2 and 8).

In the refolding process of the unfolding simulation, the peptide folded into the β-hairpin conformation by the three-step folding mechanism (Figure 9). This observation strongly supports the three-step folding mechanism for chignolin because these (re)folding events were found in three independent simulations at two different temperatures. During the folding, unfolding, and refolding processes, no intermediate states appeared; this is consistent with the results of the previous experiment.[2] Thus, chignolin was at equilibrium between the folded and unfolded states with continuous folding and unfolding transitions. Based on our unfolding simulation, we concluded that the unfolding process of chignolin is fundamentally a reversion of the three-step (re)-folding mechanism.

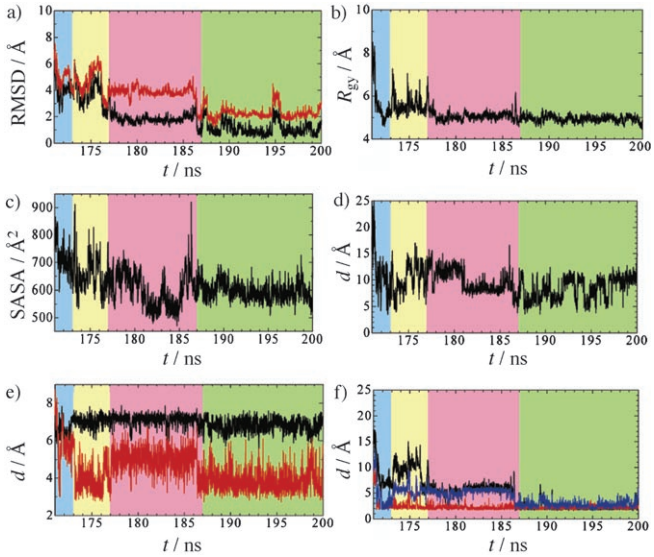

Figure 9. Results of the refolding simulation obtained from the unfolding simulation (0.171→0.200 μs). Time courses of the a) RMSDs of the main chain (black) and all atoms (red) from the solution structure, b) radius of gyration, c) SASA of the hydrophobic residues, d) distance between the two hydrophobic residues C_ξ(Tyr2) and N_ε1(Trp9), e) O(Tyr2)–N(Glu5) (corresponding to turn 2–5; black) and O(Pro4)–N(Gly7) distances (corresponding to turn 4–7; red), and f) distances between donor and acceptor atoms of the three interstrand hydrogen bonds O(Asp3)···H(Thr8) (blue), O(Asp3)···H(Gly7) (red), and H(Asp3)···O(Thr8) (black). Color regions are as in Figure 3.

Conclusions

We have observed the folding, refolding, and unfolding events of chignolin at the atomic level by using extensive all-atom MD simulations with an explicit solvent. Although there are many inconsistent explanations with regard to the folding mechanism of the β-hairpin, our findings appropri-

ately interpret the folding mechanism of chignolin as involving a combination of these explanations. The folding of chignolin begins with the hydrophobic assembly of two aromatic rings (Tyr2 and Trp9) and the formation of a nascent turn structure, which is similar to the findings of other groups.[12,23] This is also a combination of previous theories, which state that the folding begins with the formation of a turn[3,4,16,24] or hydrophobic collapse.[12,14,17–20] In the final stage of folding, the formation of the native hydrogen-bond network and the hydrophobic core as well as the arrangement of side-chain–side-chain packing occur simultaneously. This is consistent both with previous observations[15,27,30] in which the hydrophobic core and hydrogen bonds form simultaneously, and with the combination of findings that the final stage of β-hairpin folding is the formation of hydrogen bonds[12,14,17,18,20,26] or the hydrophobic core.[3,4,16,24] Furthermore, our three-step folding process is consistent with the folding process of the hairpin peptide derived from the B1 domain of the protein G as proposed by Evans and Wales,[50] in which the first step of the folding consists mainly of loosely hydrogen-bonded structures, the second is made up of compact structures with the hydrophobic core, and finally hydrogen-bond formation and hydrophobic packing occur concertedly. Our long-timescale simulations enabled the construction of a scenario for the folding process of chignolin.

Experimental Section

System Setup

We performed a series of MD simulations of chignolin (Table 1). The solution structure determined by NMR spectroscopy (PDB ID: 1UAO)[2] was used as the initial structure for the NMR and unfolding simulations. The fully extended structure (all residual dihedral angles ϕ and $\psi = 180°$) was generated as the initial structure of the folding simulation. An artificial α-helical structure was also constructed for the initial structure of the helix simulation by using the modeling software MOE (Chemical Computing Group Inc.) to clarify why chignolin has the β-hairpin instead of the helical structure. All initial structures were fully solvated by the spherical water droplets of the TIP3P water molecules.[51] The radius of the water droplet was selected such that the distance of the atoms in the peptide from the wall was greater than 15.0 Å for the NMR, folding, and helix simulations and greater than 20.0 Å for the unfolding simulation (a larger water droplet was used for the unfolding simulation because chignolin expands during the unfolding process). Each solvated system was energy-minimized prior to the production MD run. For the refolding simulation, the fully unfolded structure obtained from the unfolding simulation at 65 ns was used as the initial structure. In the folding simulation, the excess water molecules were removed after about 30 ns, when the radius of gyration (compactness) of the peptide was less than 6 Å (that of the native structure is approximately 5 Å), to reduce computational costs.

MD Simulations

All MD simulations were performed by using Amber 8.0[52] on a personal computer (Xeon 3.2 GHz) equipped with an MDGRAPE-3 board (12 chips, two Tflops).[39–41] The CPU time usage was 7.5 ns day^{-1} for the refolding simulation (10161 atoms) with MDGRAPE-3. The parm99 force field[53] was adopted, and the time step was set to 2.0 fs. All nonbonded interactions, namely, the van der Waals and Coulomb forces and energies, were calculated directly and accurately by using MDGRAPE-3. All bond lengths were constrained to equilibrium lengths by the SHAKE method.[54] Each system was gradually heated or cooled to 277 K (refolding simulation) or 373 K (unfolding simulation) during the first 46 or 62 ps (unfolding simulation) with a heating/cooling rate of 6 K ps^{-1}, and its temperature was maintained constant at 277 K by coupling to a temperature bath for the NMR, folding, refolding, and helix simulations or at 373 K for the unfolding simulation with a coupling constant of 1.0 ps.[55] During the simulations, water molecules at the edge of the water droplet were restrained by the soft harmonic potential (1.5 kcal mol^{-1} Å^{-2}) to prevent their movement away from the peptide.

Calculations of Potential of Mean Force

By using umbrella-sampling simulations, we calculated the potential of mean forces (PMFs) for the formation of turn 2–5 and turn 4–7 along the distance between the backbone oxygen atom of Tyr2 and backbone nitrogen atom of Glu5 (O(Tyr2)–N(Glu5)) for turn 2–5 and O(Pro4)–N(Gly7) for turn 4–7. The extended structure that was fully solvated and heated to 277 K was used as the initial system for the umbrella-sampling simulations. In each system, 13 umbrella-sampling windows were simulated with an interwindow spacing of 0.5 Å and a force constant of 20.0 kcal mol^{-1} Å^{-2} to ensure good overlap of the trajectories between adjacent windows. The total umbrella-sampling simulation was 13.0 ns for each system. At a separation of around 10 Å between the O and H atoms involved in the backbone hydrogen bonds, some electrostatic forces were still acting between these atoms, so the PMF profile did not become flat beyond 10 Å. However, these atoms could not be separated further because the turn structure was fully extended around that separation.

Acknowledgements

We sincerely thank Dr. S. Honda for helpful discussions. This work was supported by the contracted research "Protein 3000 Project" of the Ministry of Education, Culture, Sports, Science, and Technology of Japan.

[1] S. Honda, N. Kobayashi, E. Munekata, *J. Mol. Biol.* **2000**, *295*, 269.
[2] S. Honda, K. Yamasaki, Y. Sawada, H. Morii, *Structure* **2004**, *12*, 1507.
[3] V. Muñoz, E. R. Henry, J. Hofrichter, W. A. Eaton, *Proc. Natl. Acad. Sci. USA* **1998**, *95*, 5872.
[4] V. Muñoz, P. A. Thompson, J. Hofrichter, W. A. Eaton, *Nature* **1997**, *390*, 196.
[5] R. P. Chen, J. J. Huang, H.-L. Chen, H. Jan, M. Velusamy, C.-T. Lee, W. Fann, R. W. Larsen, S. I. Chan, *Proc. Natl. Acad. Sci. USA* **2004**, *101*, 7305.
[6] D. Du, Y. Zhu, C.-Y. Huang, F. Gai, *Proc. Natl. Acad. Sci. USA* **2004**, *101*, 15915.
[7] R. B. Dyer, S. J. Maness, E. S. Peterson, S. Franzen, R. M. Fesinmeyer, N. H. Anderson, *Biochemistry* **2004**, *43*, 11560.
[8] N. Kobayashi, S. Honda, H. Yoshii, E. Munekata, *Biochemistry* **2000**, *39*, 6564.
[9] N. N. Kuo, J. J. Huang, J. Miksovska, R. P. Chen, R. W. Larsen, S. I. Chan, *J. Am. Chem. Soc.* **2005**, *127*, 16945.
[10] S. J. Maness, S. Franzen, A. C. Gibbs, T. P. Causgrove, R. B. Dyer, *Biophys. J.* **2003**, *84*, 3874.
[11] Y. Xu, R. Oyola, F. Gai, *J. Am. Chem. Soc.* **2003**, *125*, 15388.
[12] A. R. Dinner, T. Lazaridis, M. Karplus, *Proc. Natl. Acad. Sci. USA* **1999**, *96*, 9068.
[13] O. J. Galzitskaya, J. Higo, A. V. Finkelstein, *Curr. Protein Pept. Sci.* **2002**, *3*, 191.
[14] A. E. García, K. Y. Sanbonmatsu, *Proteins* **2001**, *42*, 345.
[15] D. K. Klimov, D. Thirumalai, *Proc. Natl. Acad. Sci. USA* **2000**, *97*, 2544.
[16] A. Kolinski, B. Ilkowski, J. Skolnick, *Biophys. J.* **1999**, *77*, 2942.
[17] J. Lee, S. Shin, *Biophys. J.* **2001**, *81*, 2507.
[18] B. Ma, R. Nussinov, *J. Mol. Biol.* **2000**, *296*, 1091.

[19] P. H. Nguyen, G. Stock, E. Mittag, C. K. Hu, M. S. Li, *Proteins* **2005**, *61*, 795.
[20] V. S. Pande, D. Rokhsar, *Proc. Natl. Acad. Sci. USA* **1999**, *96*, 9062.
[21] D. Roccatano, A. Amadei, A. DiNola, H. J. C. Berendsen, *Protein Sci.* **1999**, *8*, 2130.
[22] M. M. Seibert, A. Patriksson, B. Hess, D. van der Spoel, *J. Mol. Biol.* **2005**, *354*, 173.
[23] C. D. Snow, L. Qui, D. Du, F. Gai, S. J. Hagen, V. S. Pande, *Proc. Natl. Acad. Sci. USA* **2004**, *101*, 4077.
[24] J. Tsai, M. Levitt, *Biophys. Chem.* **2002**, *101–102*, 187.
[25] G. Wei, N. Mousseau, P. Derreumaux, *Proteins* **2004**, *56*, 464.
[26] X. Wu, B. R. Brooks, *Biophys. J.* **2004**, *86*, 1946.
[27] B. Zagrobic, E. J. Sorin, V. S. Pande, *J. Mol. Biol.* **2001**, *313*, 151.
[28] J. Zhang, M. Qin, W. Wang, *Proteins* **2006**, *62*, 672.
[29] R. Zhou, B. J. Berne, R. Germain, *Proc. Natl. Acad. Sci. USA* **2001**, *98*, 14931.
[30] Y. Zhou, A. Linhananta, *Proteins* **2002**, *47*, 154.
[31] D. Satoh, K. Shimizu, S. Nakamura, T. Terada, *FEBS Lett.* **2006**, *580*, 3422.
[32] P. A. Thompson, W. A. Eaton, J. Hofrichter, *Biochemistry* **1997**, *36*, 9200.
[33] S. Williams, T. P. Causgrove, R. Gilmanshin, K. S. Fang, R. H. Callender, W. H. Woodruff, R. B. Dyer, *Biochemistry* **1996**, *35*, 691.
[34] U. Mayor, N. R. Guydosh, C. M. Johnson, J. G. Grossmann, S. Sato, G. S. Jas, S. M. Freund, D. O. Alonso, V. Daggett, A. R. Fersht, *Nature* **2003**, *421*, 863.
[35] C. D. Snow, H. Nguyen, V. S. Pande, M. Gruebele, *Nature* **2002**, *420*, 102.
[36] B. Zagrobic, C. D. Snow, M. R. Shirts, V. S. Pande, *J. Mol. Biol.* **2002**, *323*, 927.
[37] G. Jayachandran, V. Vishal, V. S. Pande, *J. Chem. Phys.* **2006**, *124*, 164902.
[38] Y. Duan, P. A. Kollman, *Science* **1998**, *282*, 740.
[39] M. Taiji, T. Narumi, Y. Ohno, N. Futatsugi, A. Suenaga, N. Takada, A. Konagaya, *Proc. Supercomputing 2003*, in CD-ROM.
[40] M. Taiji, *Proc. Hot Chips* **2004**, *16*, in CD-ROM.
[41] T. Narumi, Y. Ohno, N. Okimoto, T. Koishi, A. Suenaga, N. Futatsugi, R. Yanai, R. Himeno, S. Fujikawa, M. Ikei, M. Taiji, *Proc. Supercomputing* **2006**, in CD-ROM.
[42] K. Ikeda, J. Higo, *Protein Sci.* **2003**, *12*, 2542.
[43] C. M. Stultz, *Protein Sci.* **2006**, *15*, 2166.
[44] T. Kimura, T. Uzawa, K. Ishimori, I. Morishima, S. Takahashi, T. Konno, S. Akiyama, T. Fujisawa, *Proc. Natl. Acad. Sci. USA* **2005**, *102*, 2748.
[45] J.-E. Shea, J. N. Onuchic, C. L. Brooks III, *Proc. Natl. Acad. Sci. USA* **2002**, *99*, 16064.
[46] B. K. Ho, K. A. Dill, *PLoS Comput. Biol.* **2006**, *2*, e27.
[47] M. Ota, M. Ikeguchi, A. Kidera, *Proc. Natl. Acad. Sci. USA* **2004**, *101*, 17658.
[48] D. van der Spoel, M. M. Seibert, *Phys. Rev. Lett.* **2006**, *96*, 238102.
[49] W. Kabsch, C. Sander, *Biopolymers* **1983**, *22*, 2577.
[50] D. A. Evans, D. Wales, *J. Chem. Phys.* **2004**, *121*, 1080.
[51] W. L. Jorgensen, J. Chandrasekhar, J. D. Madura, R. W. Impey, M. L. Klein, *J. Chem. Phys.* **1983**, *79*, 926.
[52] D. A. Case, T. A. Darden, T. E. Cheatham III, C. L. Simmerling, J. Wang, R. E. Duke, R. Luo, K. M. Merz, B. Wang, D. A. Pearlman, M. Crowley, S. Brozell, V. Tsui, H. Gohlke, J. Mongan, V. Hornak, G. Cui, P. Beroza, C. Schafmeister, J. W. Caldwell, W. S. Ross, P. A. Kollman, Amber 8.0, University of California San Francisco, San Francisco (USA), **2004**.
[53] J. Wang, P. Cieplak, P. A. Kollman, *J. Comput. Chem.* **2000**, *21*, 1049.
[54] J.-P. Ryckeart, G. Ciccotti, H. J. C. Berendsen, *J. Comput. Chem.* **1997**, *23*, 327.
[55] H. J. C. Berendsen, J. M. P. Postma, W. F. van Gunsteren, A. DiNola, J. R. Haak, *J. Comput. Phys.* **1984**, *81*, 3684.

Received: November 21, 2006
Revised: February 23, 2007
Published online: April 5, 2007

